Breakthrough Analysis for Water Defluoridation Using Surface-Tailored Zeolite in a Fixed Bed Column

Maurice S. Onyango,*,† Taile Yvonne Leswifi,† Aoyi Ochieng,‡ Dalibor Kuchar,§ Fred O. Otieno,|| and Hitoki Matsuda§

Department of Chemical and Metallurgical Engineering, Tshwane University of Technology, Pretoria 0001, South Africa, School of Chemical and Metallurgical Engineering, University of the Witwatersrand, Johannesburg, South Africa, Department of Chemical Engineering, Nagoya University, Nagoya 464-8603, Japan, and Faculty of Engineering and the Built Environment, Tshwane University of Technology, Pretoria 0001-South Africa

Treatment of drinking water containing fluoride ion requires a robust and an effective technique. This can be achieved by the use of an appropriate sorption material in a fixed-bed filter. Consequently, fluoride adsorption behavior, expressed as breakthrough curve (BTC), has been investigated both in a continuous and intermittent mode of operation, using charged-reversed zeolite particles in a fixed bed filter. The fluoride concentration ranged from 5 to 20 mg/L, typical of what is found in natural systems such as groundwater. In all the fluoride removal experiments, the BTC curves were consistent with the ideal *s*-shape. A large volume of water was processed for low initial concentration of fluoride, for slow flow velocity, and for bed containing large amount of the sorption media. Equally important, no aluminum was eluted from the zeolite structure, making the sorption media safe for water treatment. A two-parameter logistic model was used to simulate the BTCs. Separately, the fingerprint of intraparticle diffusion was confirmed through operation of the fixed-bed in an intermittent mode.

1. Introduction

Fluorosis is a pandemic health problem in countries such as Kenya, Tanzania, South Africa, Ethiopia, India, and China, among others. It is mainly caused by the presence of elevated levels of fluoride ions in drinking water. Persons suffering from fluorosis manifest discolored teeth and deformed bones.[1−3] The latter is a crippling disability that has a major public health and socio-economic impact. Thus, fluoride in drinking water has attracted public health interest and has been a subject of study by several researchers.[4−7] As a consequence, many technologies for defluoridation, such as the use of membrane, ion-exchange, adsorption, coagulation, and electrochemical techniques, have been developed or are at the developmental stage.[8−10] Of these techniques, adsorption is probably the most robust, with several end-user applications, and best suited to developing countries because it is relatively lower in cost, easy to use, and can be developed to operate without necessarily using electricity.

There are a number of configurations dedicated to undertaking liquid-phase adsorption separation and purification process such as batch, fixed-bed, and fluidized bed. Over the years, the fixed bed adsorption filter has become the most commonly used configuration in drinking water treatment. The advantages of fixed bed configuration in water treatment include: inherent production of high quality drinking water, its simplicity, ease of operation and handling as well as the possibility of in situ regeneration. Moreover, the configuration is suitable for use as a point-of-use (POU) system and ideal for an individual household, especially in developing countries. In addition, the configuration can be useful as a point-of-entry (POE) system particularly in serving a small or large community as a function of water demand profile.

Several researchers have extensively studied defluoridation of drinking water using various adsorption media in a fixed-bed column. For instance, Rubel[11] as well as Ghorai and Pant[12] used activated alumina, while Mjengera and Mkongo[13] used bone char, wherein both cases the feasibility of using fixed bed configuration as a defluoridation unit was shown. In fact, bone char and activated alumina adsorption are among the few adsorption techniques described by the World Health Organization (WHO) as the best demonstrated available technology (BDAT) for remediation of fluoride-containing drinking water. However, activated alumina provides limited defluoridation because it has low adsorption capacity for fluoride. However, bone char is disapproved in some communities due to socio-cultural reasons and also because the final water quality after defluoridation process is low.[14] The above inherent limitations motivate the development of new materials characterized by high adsorption capacity for fluoride, which can be universally accepted and produce water of high quality. One such material is surface-tailored zeolite. This adsorbent is made from commercially available zeolite F9 by replacing the charge-balancing cation (typically Na^+) with Al^{3+}. Upon the exchange, the eletrokinetic property of the zeolite is altered; the charge on the surface changes from negative to positive. The positive surface charge provides sites for sorption of anions such as fluoride. We have shown in batch equilibrium studies that surface-tailored zeolite has a higher adsorption capacity for fluoride than most commercial adsorbents (see Table 1).[15−23] Moreover, it is competitive in cost.[24]

In order to design an effective adsorption separation or purification unit, preliminary design information is a critical prerequisite.[25] Often, the information is gathered through extensive series of experiments with a view to determine its optimal performance under various design and operating

* To whom correspondence should be addressed.
† Department of Chemical and Metallurgical Engineering, Tshwane University of Technology.
‡ School of Chemical and Metallurgical Engineering, University of the Witwatersrand.
§ Department of Chemical Engineering, Nagoya University.
|| Faculty of Engineering and the Built Environment, Tshwane University of Technology.

10.1021/ie0715963 CCC: $40.75
Published on Web 12/01/2008

Table 1. Batch Equilibrium Adsorption Capacities of Selected Adsorbents

adsorbent	capacity (mg/g)	source
bone char	0.3–11.4	Mwaniki [14]
Al–zeolite F9	28–41	Onyango et al. [15]
activated alumina (AA)	4.04	Maliyekkal et al. [16]
magnesia amended AA	10.1	Maliyekkal et al. [16]
Fe–Al–Ce trimetal oxide	178	Wu et al. [17]
La–CCB	4.71	Natrayasamy and Meenakshi [18]
Zn–Al-LHDs	1.14–4.16	Mandal and Mayadevi [19]
alum sludge	5.39	Sujana et al. [20]
Al_2O_3/ CNT	4.1	Li et al. [21]
ACNTs	28.7	Li et al. [22]

parameters. The operating conditions and fluid features that should be taken into account to yield a good design include; linear flow rate, initial concentrations, bed size, particle size, type of adsorbents, pH, and temperature. For the purpose of reducing costs and ultimately the number of experiments essential to acquire all the necessary priori knowledge, models are used to predict the optimal conditions via a systematic variation of the above system parameters. Models can be broadly classified as follows: mechanistic, empirical, or simplistic. Mechanistic models are extremely detailed and account for all of the fundamental mass transport mechanisms (external film, pore and surface diffusion, axial dispersion) and reaction kinetics and thus require high level expertise. In view of the above limitation, "short cut" models have been developed and are now commonly applied, such as the empty bed residence time, which is the time that the liquid would take to fill the volume of the adsorbent bed, the bed depth service time, and the two-parameter models.[26−29] These "short cut" models are tractable, have a high degree of accuracy, and involve small computation time. Moreover, they do not require high mathematical knowledge to use.

This work is a continuation of our earlier studies.[15,23] Broadly, the goal is to evaluate the surface-tailored zeolite performance with respect to drinking water defluoridation. The specific objectives are the evaluation of zeolite type, adsorbent mass, flow velocity, and initial fluoride concentration with respect to the performance indicators such as adsorbent exhaustion rate and number of bed volumes processed. The rate limiting step in fluoride adsorption is corroborated through operation of fixed bed in intermittent mode.

2. Theory of Activation of Zeolite and Zeolite−Fluoride Interaction

The structure of most zeolites is negatively charged due to isomorphic substitution of Al^{3+} for Si^{4+}. To use zeolites in anionic adsorption, their surfaces need to be tailored by altering their electrokinetic properties; making them positively charged. Tailoring of adsorbents can be done by either a wet or dry process. The wet method is often adopted, and it involves the use of an aqueous salt solution of the modifying metal. We have shown in our previous studies that treating low- or medium-silica zeolite such as A4, F9, or HSZ 300HUD with Al^{3+}, La^{3+}, or Fe^{3+} salt solution creates adsorption media with high affinities for inner sphere complexe-forming species.[15,23,30,31] Among the aforementioned salts, Al^{3+} was particularly found to create adsorption media with high capacity and specificity for fluoride. If zeolite F9 is taken for illustrative purposes, the Na^+-bound zeolite is exchanged with Al^{3+} from aqueous solution (see Figure 1) creating a surface-tailored zeolite F9 adsorption media with pH of point-of-zero charge (pH_{pzc}) of 8.15.[15] The reaction proceeds as follows:

$$Al^{3+}(soln) + 3Na^{+}(zeo) \leftrightarrow Al^{3+}(zeo) + 3Na^{+}(soln)$$

The aluminum is bound onto the *o*-plane in the zeolite. In solution at $pH < pH_{pzc}$, protonated sites dominate according to the following reaction:

$$\equiv AlOH(\text{neutral sites}) + H^{+} \leftrightarrow \equiv AlOH_2^{+} + (\text{protonated sites})$$

Fluoride adsorbs on either the neutral (≡AlOH) or protonated ($\equiv AlOH_2^+$) sites as shown in Figure 2. The mechanism of fluoride sorption is by ion exchange and inner-sphere complexation.[24,25]

3. Materials and Methods

3.1. Materials. The sodium fluoride, aluminum sulfate, and zeolite F9 granular particles used in this study were supplied by Wako Chemicals, while zeolite HUD 300HSZ was donated by Tosoh Chemicals, Japan. To make surface-tailored zeolite for fixed-bed adsorption studies, 50 g zeolite F9 (Na^+ form; Si/Al ratio: 1.23; pore size: 9Å; BET: 232 m^2/g) or HSZ 300HUD(H^+ form, Si/Al ratio:2.75−3.25; BET: 1054 m^2/g) was added to 1 L of 0.075 M aluminum sulfate solution. The mixture was stirred for 2 days and then washed several times using demineralised water to lower the electrical conductivity. Finally, the modified zeolite was air-dried at room temperature for 2 days. The zeolites prepared in this manner are hereafter referred to as Al−F9 for F9 zeolite and Al-HUD for HSZ 300HUD zeolite. The exchange of sodium from the zeolite structure with aluminum from the aqueous solution was qualitatively verified using Energy Dispersive X-ray Spectrometer (EDXS) (JED 2140-JEOL) while inductively coupled plasma-mass spectrometry (ICP-MS) was used to determine the quantitative exchange and elemental composition of the zeolites. The former and the latter were previously reported.[15,23] The surface morphology of both zeolites was explored by scanning electron microscopy (SEM).

3.2. Experimental Section. 3.2.1. Fixed-Bed Adsorption Filter Set Up. Figure 3 shows the experimental setup used in this study. A pyrex glass column with an internal diameter of 2.1 cm and a total height of 15 cm was used as an adsorption column. The zeolite adsorbent was packed between glass wool while inert beads were placed at the bottom and top ends. The fluoride ion spiked solution, contained in a magnetically stirred container at an appropriate concentration, was pumped vertically upward inside the column. The flow velocity was observed periodically by collecting 100 mL of the exiting solution and recording the time taken for the given volume. The effect of several variables, such as bed mass, initial fluoride ion concentration, flow velocity, and intermittent operation were studied. Samples used for determining the residual fluoride content were taken at time intervals ranging from 30 to 60 min, until the fluoride ion concentration in the effluent was nearly the same as the initial concentration. This procedure facilitated the determination of breakthrough curves (BTC).

The bed capacity at breakthrough point (1.5 mgF/L) was determined from the expression

$$q_b = \frac{C_o}{m}\int_0^{V_b}\left(1 - \frac{C_t}{C_o}\right)dV \qquad (1)$$

where q_b is bed capacity at breakthrough point (mg/g), m is the bed mass (g), C_o is the initial concentration (mg/L), C_t is the concentration in the exit stream at any time, and V_b is the volume processed at breakthrough point.

3.2.2. Analysis. The residual fluoride concentration was measured by fluoride ion selective electrode (Horiba ltd,

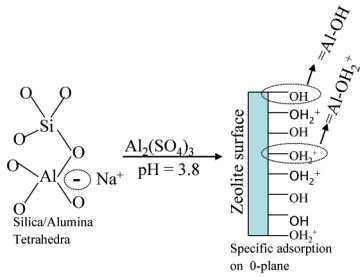

Figure 1. Activation of zeolite with Al^{3+} salt solution.

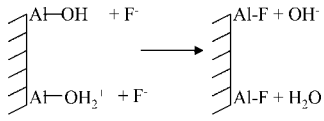

Figure 2. Zeolite−fluoride interaction: Formation of inner-sphere complexes.

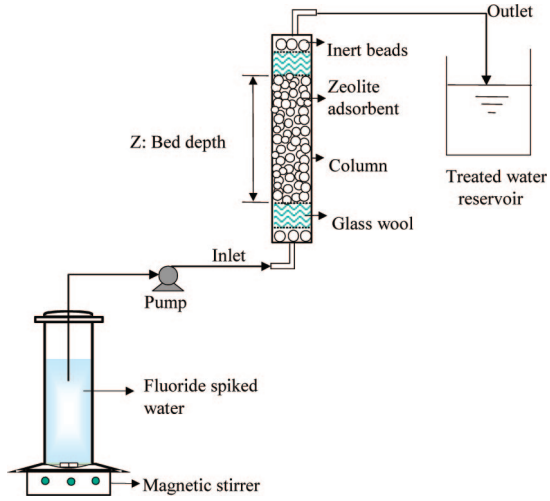

Figure 3. Experimental set up for water defluoridation in zeolite fixed-bed column.

Japan: limit of detection = 0.02 mg/L) in accordance with the Japanese standard method (JIS K0102). Accordingly, a calibration curve was initially prepared by recording the potential values for a range of known fluoride concentration, mostly 0.1 to 5 mg/L. For the determination of fluoride concentration above this range, appropriate dilution was done. To ensure that there was no interference during fluoride measurements, Total Ionic Adjustment Buffer (TISAB, pH 5.3) solution containing 58 g NaCl, 1 g diammonium hydrogen citrate, 50 mL acetic acid, and an appropriate amount of 5 M NaOH all in a volume of 1 L, was used during fluoride ion concentration measurements.

The dissolution of aluminum from the zeolite structure was monitored by measuring the residual concentration of aluminum in the effluent from the column (see Figure 3), using inductively coupled plasma atomic emission spectrophotometer (ICP-AES: SpectroCiros CCD, Germany). The sodium content of the effluent from the column was also determined.

3.3. Performance Indicators. In water treatment, fixed beds are usually operated with an objective to reduce the concentration of a given contaminant to a value below the maximum allowable concentration. The total cost of the fixed bed is determined by the volume of the bed and size of the column. For a given adsorbent bed mass, the adsorption performance is directly related to the number of bed volumes processed

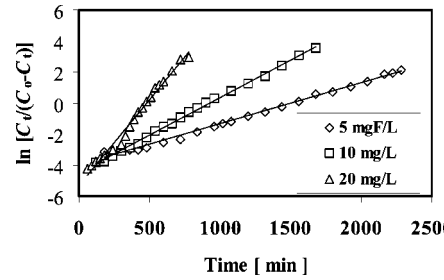

Figure 4. Plot of two-parameter logistic model.

before the breakthrough point is reached. The number of bed volumes is given by the following:

$$\text{number of bed volumes (BV)} = \frac{\text{volume of water treated at breakthrough point, } L}{\text{volume of adsorbent bed, } L} \quad (2)$$

During operation, the adsorbent is deactivated. The rate of the deactivated will determine the frequency by which the adsorbent is replaced and hence the operating costs. The rate of deactivation is expressed as adsorbent exhaustion rate (AER), which is defined as the mass of adsorbent deactivated per volume of water treated at breakthrough point and is given by the following:

$$\text{adsorbent exhaustion rate (AER)} = \frac{\text{mass of adsorbent, } g}{\text{volume of water treated, } L} \quad (3)$$

From the foregoing discussion, low values of AER imply good performance of the bed. In section 4, AER will be the main performance indicator for comparing different operating conditions unless stated otherwise.

4. Results and Discussion

4.1. Breakthrough Analysis. Operating parameters, namely, the bed mass, flow velocity, and initial feed concentration, are the most crucial in column design. In this study, the effects of these parameters as well as those of zeolite type and intermittent operation on the removal of fluoride by surface-tailored zeolites were investigated.

4.1.1. Modeling of Breakthrough Curves Using Two-Parameter Logistic Model. The flow and mass transfer in adsorption column is described by complex nonlinear differential equations that involve a number of parameters. In recent years, several researchers have developed "short cut" models that are tractable, match experimental and model data satisfactorily well, and involve small computation time. This work considers a two parameter logistic model expressed as follows:[28]

$$\ln\left(\frac{C_t}{C_o - C_t}\right) = k(t - \tau) \quad (4)$$

where k (min^{-1}) is the rate constant and is a measure of the slope of breakthrough curves. Steeper breakthrough curves have higher values of k. The parameter, τ (min), represents the time at which the exit concentration equals to 50% of the initial concentration. To determine the values of k and τ, plots of ln $[C_t/(C_o - C_t)]$ versus t are constructed and from the slopes of such plots, the k parameter is obtained, while τ is obtained from the intercept of the plots (see Figure 4 for illustration).

Table 2 lists the model parameters. The regression coefficient values suggest that the model fits the data points satisfactorily well.

Table 2. Summary of Logistic Model Parameters of Zeolite Column for Water Defluoridation

	rate constant k (min^{-1})	sorption time at $C_o/2$ τ (min)	R^2
	zeolite type		
Al−F-9	0.0049	920.0	0.9975
Al-HUD	0.0066	802.9	0.9869
	adsorbent mass (g)		
8.20	0.0068	562.3	0.9917
12.3	0.0049	920.0	0.9975
16.4	0.0041	1205.1	0.9845
	initial concentration (mg/L)		
5	0.0026	1537.6	0.9950
10	0.0049	920.0	0.9975
20	0.0109	484.1	0.9864
	flow velocity (cm/s)		
3.29×10^{-2}	0.0041	1148.7	0.9918
4.87×10^{-2}	0.0049	920.0	0.9975
8.20×10^{-2}	0.0075	584.0	0.9667

Table 3. Summary of Pertinent Results at Breakthrough Point

	service time, t_b (min)	capacity, q_b (mg/g)	bed volumes processed	AER (g/L)
	zeolite type			
Al−F-9	573	4.64	557	2.1
Al−HUD	608	4.66	330	2.1
	adsorbent mass (g)			
8.20	310	3.72	448	2.7
12.3	573	4.64	557	2.1
16.4	830	4.79	599	2.0
	flow velocity (cm/s)			
3.29×10^{-2}	780	4.10	512	2.3
4.87×10^{-2}	573	4.64	557	2.1
8.20×10^{-2}	347	4.59	567	2.1
	initial concentration (mg/L)			
5	1211	3.79	1177	1.0
10	573	4.64	557	2.1
20	308	4.93	300	3.8

4.1.1. Effect of Zeolite-Type on BTC. Each column had the same mass (12.3 g) of the adsorption media and the influent concentration of fluoride was fixed at 10 mgF/L. Figure 5 shows the effluents histories of fluoride for unmodified and two modified zeolite sorbents. Unmodified zeolite has poor affinity for fluoride due to its inherent negatively charged structure and is not considered for further discussion. Both modified zeolite sorbents somehow exhibit similar behavior. As a consequence, there is no large difference (see Table 3) in the service time (t_b), sorbent capacity (q_b), and the AER at breakthrough concentration of 1.5 mgF/L(WHO guideline for drinking water). Furthermore, the volume of water processed at the breakthrough point is closely the same at 5.90 and 5.79 L for Al-HUD and Al−F9 zeolites, respectively. In terms of the number of bed volumes (BV), up to 330 BV were processed for Al-HUD and up to 557 BV were processed for Al−F9 at breakthrough point. The difference in the BV values for the two zeolites inheres in their difference in physical properties. Al−F9 zeolite has a higher density than Al-HUD zeolite[29] and consequently, for the same amount of the media, Al−F9 zeolite occupies advantageously smaller volume. When the slopes of the BTCs are considered, it is observed that the one for Al-HUD is slightly steeper than that for Al−F9. This is further confirmed by the numerical k value (Table 2) predicted by the two-parameter logistic model, which is higher for Al-HUD than for Al−F9. The time required for the initial concentration to reduce by a factor of 0.5, τ, however is higher for Al−F9 than for Al-HUD. Sorption in zeolites takes place in the microparticles matrix where the active sites are located. A scanning electron microscopy (SEM) study (Figures 6, parts a and b) of the two zeolites reveals that the microparticles of Al-HUD zeolite are smaller than those of Al−F9 zeolite. Kinetically, this implies that the transport of fluoride ions to the active sites of Al-HUD zeolite is faster than that to the active sites of Al−F9 zeolite due to reduced intraparticle diffusion resistance. Thus, beyond the breakthrough point, the consequence of reduced diffusion resistance to mass transfer is a steep breakthrough curve (for Al-HUD). Using the number of bed volumes processed as a performance indicator, Al−F9 zeolite adsorbent was chosen and used in the subsequent experiments.

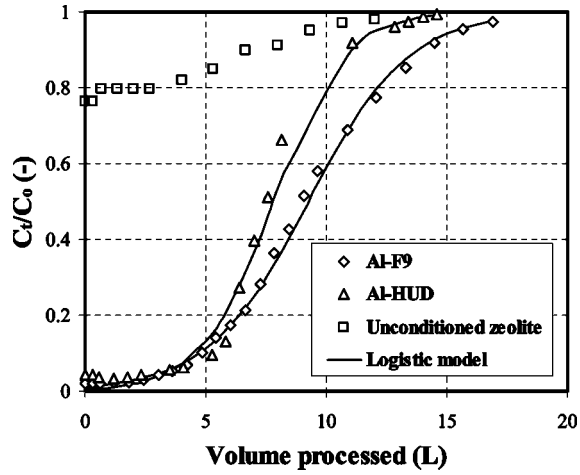

Figure 5. Breakthrough curves for fluoride sorption onto unconditioned, Al−F9 and Al−HUD zeolites. Initial fluoride concentration = 10 mg/L, adsorbent mass = 12.3 g, adsorbent particle size = 0.15−0.30 mm, pH = 6.4, flow velocity = 4.87×10^{-2} cm/s, temperature = 295.6 K.

4.1.2. Effect of Adsorbent Mass. By fixing the initial solute concentration and flow velocity, the variation of bed mass determines the number of active sites available for sorption and the contact time of solute with the adsorbent. In this experimental run, the initial fluoride concentration and the flow velocity were fixed at 10 mg/L and 4.87×10^{-2} cm/s, respectively. As a result of the variation of the bed mass, the empty bed contact time varied from 0.69 to 1.39 min.

Figure 7 shows the BTC obtained upon varying the quantity of adsorption media (Al−F9) between 8.2 and 16.4 g. From the BTCs, the t_b and q_b were determined and are summarized in Table 3. The t_b and q_b values increase with an increase in sorbent mass. The volumes of water treated at breakthrough point (corresponding to $C/C_0 = 0.15$) were found to be 3.04, 5.79, and 8.31 L, for 8.2, 12.3, and 16.4 g beds, respectively. As a result, the corresponding bed volumes were 448, 557, and 599 for 8.2, 12.3, and 16.4 g beds, while the computed AER values were found to be 2.7, 2.1, and 2.0 g/L for the 8.2, 12.3, and 16.4 g beds, respectively. Lower values of AER signify better performance. Consequently, results of this study suggest that beds with large amounts of adsorbent are more preferable in order to yield optimal results during the adsorption process. One plausible reason for the improved performance as the bed mass was raised is that contact time, which allows for species diffusion into the internal adsorbent matrix, is increased as the bed mass is raised. The logistic model parameter k decreases while τ increases with an increase in the quantity of adsorption media. The shape of BTC and hence k should not depend on bed mass. The trend in k is anomalous but may be explained by the fact that diffusional effect on fluoride sorption was significant.

4.1.3. Effect of Flow Velocity. The column was fed with fluoride-spiked water in an upward flow mode. The average flow velocity used in this study was 3.29×10^{-2}, 4.87×10^{-2}, and 8.20×10^{-2} cm/s. The BTCs are shown in Figure 8 from which the t_b and q_b were determined. The t_b decreases but q_b shows

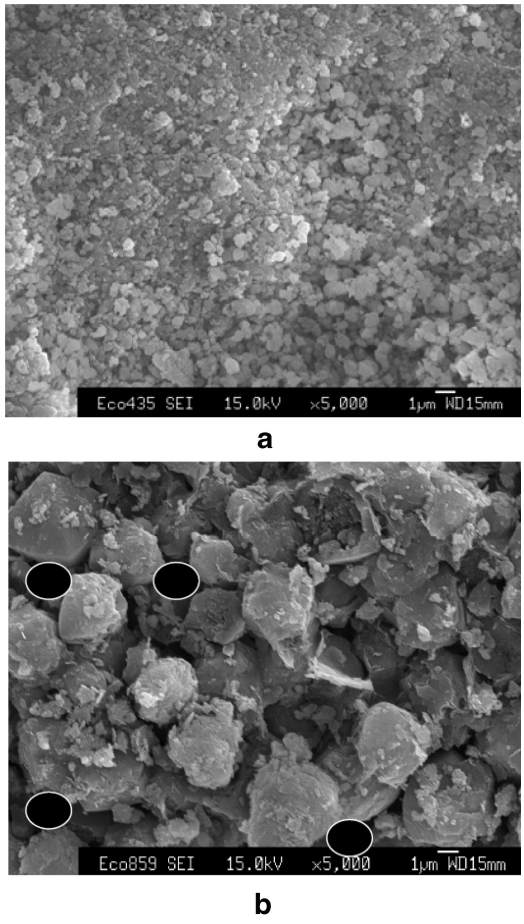

Figure 6. (a) SEM map of zeolite Al-HUD. (b) SEM map of Al−F9. Macropores are shown by circles.

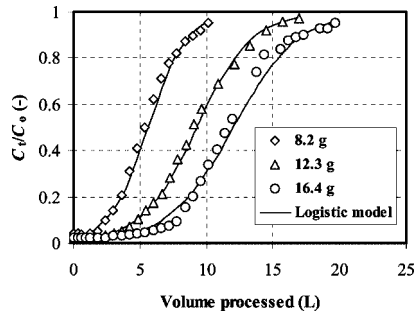

Figure 7. Breakthrough curves for fluoride sorption onto Al−F9 zeolite at different masses. Initial fluoride concentration = 10 mg/L, particle size = 0.15−0.30 mm, flow rate = 4.87×10^{-2} cm/s, pH = 6.4, and temperature = 295.6 K.

no specific trend with an increase in flow velocity. When the different volumes (BV in parenthesis) of water processed at breakthrough point were determined, it was found that 5.33(512), 5.79(557), and 5.90(567) L for 3.29×10^{-2}, 4.87×10^{-2}, and 8.20×10^{-2} cm/s, respectively, were achieved. The increase in volume processed with an increase in velocity can be attributed to reduced influence of external mass transfer resistance. The AER values obtained owing to the variation of flow rate were 2.3, 2.1, and 2.1 g/L at the flow velocity of 3.29×10^{-2}, $4.87 \times 10^{-2,}$ and 8.20×10^{-2} cm/s, respectively, showing minor influence between the two latter velocities. Table 2 shows the values of k increase and τ decrease with an increase in flow velocity. A plot of effluent concentration vs time (not shown) for various flow velocities from which the model parameters were determined, showed that equilibrium concentration (equivalent to initial concentration) was approached faster for higher flow velocity than for lower velocity. Hence k increases with an increase in flow velocity.

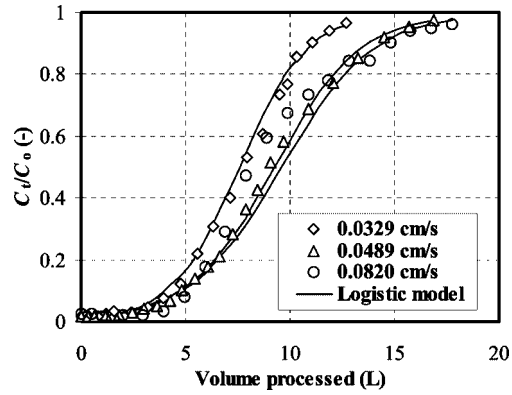

Figure 8. Breakthrough curves for fluoride sorption onto Al−F9 zeolite at different flow rates. Initial fluoride concentration = 10 mg/L, particle size = 0.15−0.30 mm, adsorbent mass = 12.3 g, pH = 6.4, temperature = 295.6 K.

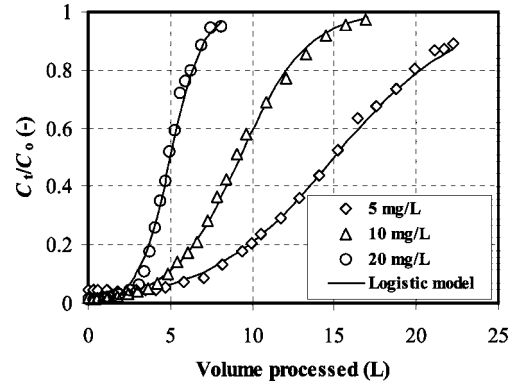

Figure 9. Breakthrough curves for fluoride sorption onto F9 zeolite at different initial concentrations. Flow rate = 0.0487 cm/s, adsorbent mass = 12.3 g, particle size = 0.15−0.30 mm, pH = 6.4, temperature = 295.6 K.

The results of this study show that the higher the flow velocity, the better the column performance. However, it was observed that the bed started to move at the highest flow velocity of 8.20×10^{-2} cm/s. This may compromise the quality of the treated drinking water due to particle attrition.

4.1.4. Effect of Initial Concentration. Three different initial concentrations of 5, 10, and 20 mg/L were used in this study. The values were chosen because they were considered to fairly represent fluoride concentration range in most groundwaters around the world. In determining the effect of initial concentration, the bed mass and flow velocity were fixed at 12.3 g and 4.87×10^{-2} cm/s, respectively. The BTCs obtained from the experimental investigations of the effect of the initial concentration on fluoride removal are depicted in Figure 9. Some of the salient features shown in Figure 9 are as follows: (i) the volume processed before a given effluent concentration is reached increases with a decrease in initial concentration and (ii) the slopes of the BTC increase with an increase in initial concentration. As a consequence of the latter, the k value was found to increase with an increase initial concentration while τ showed a reverse trend. Meanwhile, more fluoride was adsorbed (see q_b values in Table 3) at higher initial concentration due to availability of unlimited active sites on the sorption media at the prevailing experimental condition. The volumes of water treated at breakthrough point were found to be 11.87, 5.79, and 3.20 L, for 5, 10, and 20 mg/L, respectively. From the volumes

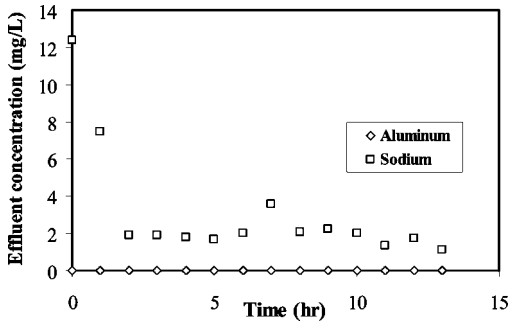

Figure 10. Elution curves for Al^{3+} and Na^{+}. Adsorbent mass = 12.3 g, particle size = 0.15−0.30 mm, flow velocity = 4.87×10^{-2} cm/s, pH = 6.4, temperature = 295 K.

processed at breakthrough point, the AER (BV in parenthesis) values were computed and found to be 1.0(1177), 2.1(557), and 3.8 (300) g/L for the initial concentrations of 5, 10, and 20 mg/L, respectively. During adsorption process, the initial concentration of a solute affects the rate of consumption of the active sites. As the concentration increases, the driving force for adsorption increases and the active sites are consumed faster. This leads to the treatment of a smaller volume of water per unit mass of adsorbent, as depicted by the large AER value. Similar trends as those presented in Figure 9 have been presented for fluoride sorption.[34]

4.2. Aluminum Level in Treated Water. Aluminum has been shown to be a neurotoxic compound if it is allowed to enter the bloodstream and is a potential cause of Alzheimer's disease. For this reason, the maximum allowable concentration in drinking water is set at 0.2 mg/L. Since zeolite was chemically modified with aluminum, the possibility of aluminum dissolution from the zeolite structure can pose a health hazard. Thus,the level of aluminum was monitored in the treated water. The bed mass was fixed at 12.3 g, pH = 6.4 and flow velocity at 4.87×10^{-2} cm/s. The breakthrough results of aluminum and sodium ions are shown in Figure 10. Aluminum ion was not detected (detection limit 0.0157 mg/L) in water suggesting that it was strongly bound onto the zeolite structure. The sodium ions, which are loosely bound onto the zeolite structure, were transferred to the solution. Given that acceptable drinking water pH ranges from 6.5 to 8.5, the modified zeolite (according to the manufacture, the structure of zeolite may collapse at pH above 12) used in this study is safe for use in treating drinking water.

4.3. Fingerprint of Diffusion-Controlled Fluoride Adsorption. Among the objectives of this study was to confirm the step in adsorption that had the most significant influence on the overall process. We recall that in the adsorption process, there are 3 main steps: (i) external diffusion, (ii) intraparticle diffusion, and (iii) surface reaction. In most adsorption processes, intraparticle diffusion plays a rate-controlling role.[36] As suggested by Faust and Aly for porous adsorbents,[37] results obtained from fixed-beds operated intermittently give full proof of an internal diffusion-controlled process. Figure 11 illustrates a plot of effluent concentration against bed volumes processed during intermittent operation. It is evident that when the operation was stopped for 12 h, the effluent concentration immediately after the resumption of the operation dropped as a result of improved performance of the bed.

In an adsorption process, concentration gradients ($\Delta q/\Delta r$) are attenuated (for a hypothetical illustration, see an inset plot in Figure 11) in the sorbent phase during progression of the experiment. The period during which the operation is interrupted allows the sorbate to be adsorbed onto the sorption

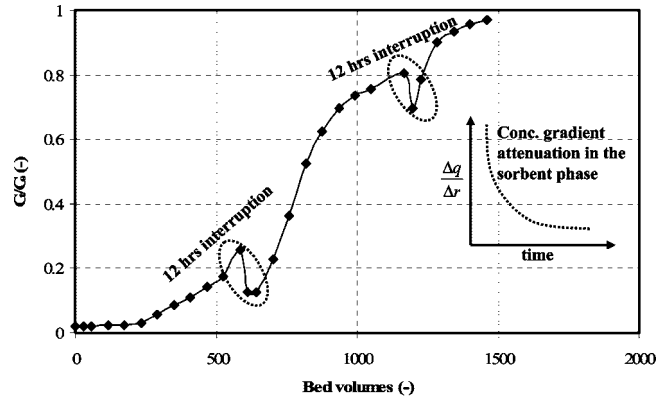

Figure 11. Breakthrough curve for fluoride sorption onto Al−F9 zeolite under intermittent operation. Initial fluoride concentration = 10 mg/L, adsorbent mass = 12.3 g, particle size = 0.15−0.30 mm, flow velocity = 4.87×10^{-2} cm/s, pH = 6.4, temperature = 295 K.

sites,[38] that is, the fluoride ions are redistributed within the pores of the adsorbent during the interrupted period. This lowers the sorbent phase concentration, ultimately creating a larger gradient in the internal matrix of the sorbent.[30,39] Immediately, the flow is resumed, and a greater adsorption rate than before flow interruption[37] is encountered, leading to a drop in effluent concentration, as shown in Figure 11 for the present fluoride−zeolite system. This behavior is a fingerprint of intraparticle diffusion controlled adsorption process. Such a conclusion was also drawn by DeMarco et al.[40] and Li and Sengupta.[39] The reason for the dominance of intraparticle diffusion in fluoride adsorption can be explained by considering the length of the diffusion path over which adsorbing species has to be transported. During the passive transport of an adsorbing species from bulk solution to the surface of an adsorption media, the resistance to mass transfer is not large since the film boundary layer is very small in comparison to the intraparticle diffusion path (up to half the radius of sorbent for active sites located near the sorbent core) a species has to move to reach the active sites. Since adsorbing species (fluoride) interact with each other and the surface of the adsorption media, the longer intraparticle diffusion path imparts increased resistance to mass transfer. This phenomenon is responsible for the dominance of intraparticle diffusion in fluoride adsorption.

5. Conclusions

Fluoride removal in a fixed bed zeolite column was investigated as a function of the zeolite type, quantity of sorbent, initial concentration, flow velocity, and intermittent operation. Experimental data confirmed a faster approach to equilibrium (equivalent to initial concentration) and a lower fluoride removal when the mass of the sorption media was low, and when flow rate and initial concentrations of fluoride were high. In further assessing the BTCs, the adsorbent exhaustion rate (AER), and number of bed volumes (BV) processed at breakthrough point were defined as the performance indicators. Low values of AER and large BV, which indicate good performance, was observed at reduced initial concentration, increased flow velocity, and adsorbent bed mass. This work also considered mathematical interpretation of the experimental results. For this, a two-parameter logistic model that is empirical, tractable, and with small computation time, and exhibiting a good match between experimental and model data points, was presented. From the model, a rate parameter was determined and discussed in relation to changes in the process variables. Considering the BTC

behavior during intermittent fixed-bed operation, it can be concluded that mass transfer in the internal matrix of zeolite was the slowest step in fluoride adsorption. Meanwhile, considering the large BV processed before breakthrough and the fact that aluminum is strongly bound on zeolite, it can be confirmed that surface-tailored zeolite is a potential and safe adsorption media for effective water defluoridation.

6. Nomenclature

Co = initial concentration of fluoride [mg/L]

C_t = column effluent concentration at any time [mg/L]

k = rate constant defined in eq 2 [min^{-1}]

m = mass of sorbent

q_b = amount of fluoride sorbed on the adsorbent at breakthrough point of 1.5 mg/L[mg/g]

t = service time [min]

V_b = volume processed at breakthrough point [L]

τ = the time at which the exit concentration equals to 50% of the initial concentration [min]

Acknowledgment

One of the authors, M.S.O., acknowledges the fellowship provided by the Japanese Ministry of Education, Science, Culture and Sports.

Literature Cited

(1) Ayoob, S.; Gupta, A. K. Fluoride in Drinking Water: A Review on the Status and Stress Effects. *Environ. Sci. Technol.* **2006**, *36*, 433.

(2) Tamer, M. N.; Köroğlu, B. K.; Arslan, Ç.; Akdoğan, M.; Köroğlu, M.; Çam, H.; Yildiz, M. Osteosclerosis Due to Endemic Fluorosis. *Sci. Total Environ.* **2007**, *373*, 43.

(3) Yoshimura, K.; Nakahashi, T.; Saito, K. Why Did the Ancient Inhabitants of Palmyra Suffer Fluorosis. *J. Archaeol. Sci.* **2006**, *33*, 1411.

(4) Harinarayan, C. V.; Kochupillai, N.; Madhu, S. V.; Gupta, N.; Meunier, P. J. Fluorotoxic Metabolic Bone Disease: An Osteo-Renal Syndrome Caused by Excess Fluoride Ingestion in the Tropics. *Bone* **2006**, *39*, 907.

(5) Misra, A. K.; Mishra, A. Study of Quaternary Aquifers in Ganga Plain, India: Focus on Groundwater Salinity, Fluoride and Fluorosis. *J. Hazard. Mater.* **2007**, *144*, 438.

(6) Xiong, X. Z.; Liu, J. L.; He, W. H.; Xia, T.; He, P.; Chen, X. M.; Yang, K. D.; Wang, A. G. Dose-Effect Relationship Between Drinking Water Fluoride Levels and Damage to Liver and Kidney Functions in Children. *Environ. Res.* **2007**, *103*, 112.

(7) Zhu, C.; Bai, G.; Liu, X.; Li, Y. Screening High-Fluoride and High-Arsenic Drinking Waters and Surveying Endemic Fluorosis and Arsenism in Shaanxi Province in Western China. *Water Res.* **2006**, *40*, 3015.

(8) Meenakshi, S.; Viswanathan, N. Identification of Selective Ion-Exchange Resin for Fluoride Sorption. *J. Colloid Interface Sci.* **2007**, *308*, 438.

(9) Shen, F.; Chen, X.; Gao, P.; Chen, G. Electrochemical Removal of Fluoride Ions from Industrial Wastewater. *Chem. Eng. Sci.* **2003**, *58*, 987.

(10) Tahaikt, M.; El Habbani, R.; Ait Haddou, A.; Achary, I.; Amor, Z.; Taky, M.; Alami, A.; Boughriba, A.; Hafsi, M.; Elmidaoui, A. Fluoride Removal from Groundwater by Nanofiltration. *Desalination* **2007**, *212*, 46.

(11) Rubel Jr, F. The Removal of Excess Fluoride from Drinking Water by the Activated Alumina Method. In *Fluoride Effects on Vegetation, Animals and Humans*; Shupe, J. L., Peterson, H. B., Leone, N. C., Eds.; Paragon Press: Salt Lake City, 1983; pp 345−349.

(12) Ghorai, S.; Pant, K. K. Investigations on the Column Performance of Fluoride Adsorption by Activated Alumina in a Fixed-Bed. *Chem. Eng. J.* **2004**, *98*, 165.

(13) Mjengera, H.; Mkongo, G. Appropriate Deflouridation Technology for Use in Flourotic Areas in Tanzania. *Phys. Chem. Earth.* **2003**, *28*, 1097.

(14) Mwaniki, D. L. Fluoride Sorption Characteristics of Different Grades of Bone Charcoal, Based on Batch Tests. *J. Dent. Res.* **1992**, *71*, 1310.

(15) Onyango, M. S.; Kojima, Y.; Aoyi, O.; Bernardo, E. C.; Matsuda, H. Adsorption Equilibrium Modeling and Solution Chemistry Dependence of Fluoride Removal from Water by Trivalent-Cation-Exchanged Zeolite F-9. *J. Colloid Interface Sci.* **2004**, *279*, 341.

(16) Maliyekkal, S. M.; Shukla, S.; Philip, L.; Nambi, I. M. Enhanced Fluoride Removal from Drinking Water by Magnesia-Amended Activated Alumina Granules. *Chem. Eng. J* **2008**, *140*, 183.

(17) Wu, X.; Yu Zhang, Y.; Dou, X.; Min Yang, M. Fluoride Removal Performance of a Novel Fe-Al-Ce Trimetal Oxide Adsorbent. *Chemosphere* **2007**, *69*, 1758.

(18) Viswanathan, N.; Meenakshi, S. Enhanced Fluoride Sorption Using La(III) Incorporated Carboxylated Chitosan Beads. *J. Colloid Interface Sci.* **2008**, *322*, 375.

(19) Mandal, S.; Mayadevi, S. Adsorption of Fluoride Ions by Zn-Al Layered Double Hydroxides. *Appl. Clay Sci.* **2008**, *40*, 54.

(20) Sujana, M. G.; R. Thakur, R. S.; Rao, S. B. Removal of Fluoride from Aqueous Solution by Using Alum Sludge. *J. Colloid Interface Sci.* **1998**, *206*, 94.

(21) Li, Y.-H.; Wang, S.; Cao, A.; Zhao, D.; Zhang, X.; Xu, C.; Luan, Z.; Ruan, D.; Liang, J.; Wu, D.; Wei, B. Adsorption of Fluoride from Water by Amorphous Alumina Supported on Carbon Nanotubes. *Chem. Phys. Lett.* **2001**, *350*, 412.

(22) Li, Y.-H.; Wang, S.; Zhang, X.; Wei, J.; Xu, C.; Luan, Z.; Dehai Wu, D. Adsorption of Fluoride from Water by Aligned Carbon Nanotubes. *Mater. Res. Bull.* **2003**, *38*, 469.

(23) Onyango, M. S.; Kojima, Y.; Kumar, A.; Kuchar, D.; Mitsuhiro, K.; Matsuda, H. Uptake of Fluoride by Al^{3+}-Pretreated Low-Silica Synthetic Zeolites: Adsorption Equilibria and Rate Studies. *Sep. Sci. Technol.* **2006**, *41*, 683.

(24) Gupta, V. K.; Ali, I.; Saini, V. K. Defluoridation of Wastewaters Using Waste Carbon Slurry. *Water Res.* **2007**, *41*, 3307.

(25) Ko, D. C. K.; Porter, J. F.; McKay, G. A Correlation-Based Approach to the Optimisation of Fixed-Bed Sorption Units. *Ind. Eng. Chem. Res.* **1999**, *38*, 4868.

(26) Bohart, G. S.; Adams, E. Q. Some Aspects of the Behavior of Charcoal with Respect to Chlorine. J. Chem. Soc. 1920, *523*.

(27) Belter, P. A.; Cussler, E. L.; Hu, W. -S. *Bioseparations: Downstream Processing for Biotechnology*; Wiley: New York, 1988.

(28) Lin, S. H.; Liu, J. M. Hydrofluoric Acid Recovery from Waste Semiconductor Acid Solution by Ion Exchange. *J. Environ. Eng.* **2003**, *129*, 472.

(29) Chu, K. H. Improved Fixed Bed Models for Metal Biosorption. *Chem. Eng. J.* **2004**, *97*, 233.

(30) Onyango, M. S.; Matsuda, H.; Ogada, T. Sorption Kinetics of Arsenic onto Iron-Conditioned Zeolite. *J. Chem. Eng. Jpn.* **2003**, *36*, 477.

(31) Onyango, M. S.; Kuchar, D.; Kubota, M.; Matsuda, H. Adsorptive Removal of Phosphate Ions from Aqueous Solution Using Synthetic Zeolite. *Ind. Eng. Chem. Res.* **2007**, *46*, 895.

(32) Harrington, L. F.; Cooper, E. M.; Vasudevan, D. Fluoride Sorption and Associated Aluminum Release in Variable Charge Soils. *J. Colloid Interface Sci.* **2003**, *267*, 302.

(33) Sathish, R. S.; Raju, A. G.; Rao, G. N.; Janardhana, C. A Fluorescent Fluoride Ion Probe Based on a Self-Organized Ensemble of 5-Hydroxyflavone-Al(III) Complex. *Spectrochim. Acta A* **2008**, *69*, 282.

(34) Sarkar, M.; Banerjee, A.; Pramanick, P. P.; Sarkar, A. R. Use of Laterite for the Removal of Fluoride from Contaminated Drinking Water. *J. Colloid Interface Sci.* **2006**, *302*, 432.

(35) Al-Muhtaseb, S. A.; El-Naas, M. H.; Abdallah, S. Removal of Aluminum from Aqueous Solutions by Adsorption on Date-Pit and BDH Activated Carbons. *J. Hazard. Mater.* **2008**, *158*, 300.

(36) Onyango, M. S.; Kojima, Y.; Kuchar, D.; Osembo, S. O.; Matsuda, H. Diffusion Kinetic Modeling of Fluoride Removal from Aqueous Solution by Charge-Reversed Zeolite Particles. *J. Chem. Eng. Jpn.* **2005**, *38*, 701.

(37) Faust, S. D.; Aly, O. M. *Adsorption Processes for Water Treatment*; Butterworth Publishers: Boston, 1987.

(38) Tran, Y. T.; Bajracharya, K.; Barry, D. A. Anomalous Cadmium Adsorption in Flow Interruption Experiments. *Geoderma.* **1998**, *84*, 169.

(39) Li, P.; Sengupta, A. K. Intraparticle Diffusion During Selective Ion Exchange with a Macroporous Exchanger. *React. Funct. Polym.* **2000**, *44*, 273.

(40) DeMarco, M. J.; SenGupta, A. K.; Greenleaf, J. E. Arsenic Removal Using a Polymeric/Inoganic Hybrid Sorbent. *Water Res.* **2003**, *37*, 164.

Received for review November 24, 2007
Revised manuscript received October 16, 2008
Accepted October 16, 2008

IE0715963